

# Optically Transparent Dual-Band MIMO Antenna Using Micro-Metal Mesh Conductive Film for WLAN System

Q. L. Li, S. W. Cheung, *Senior Member, IEEE*, Di Wu, and T. I. Yuk, *Member, IEEE*

**Abstract**—An optically transparent dual-band multiple-input-multiple-output (MIMO) antenna designed using a micro-metal mesh conductive (MMMC) film for the wireless local area network applications is presented. The antenna consists of two meandered-monopole radiators that are microstrip-fed. The MMMC film is constructed by Cima NanoTech using SANTE self-assembling nanoparticle technology and has a high transmittance of above 75% and a low sheet resistance of  $0.05 \Omega/\text{sq}$ . The antenna is cut from an MMMC film and glued on a glass substrate with a thickness of 1.09 mm. A layer of MMMC film is glued on the other side of the substrate to serve as ground. The antenna is studied and designed using computer simulation, and the prototyped antenna is measured using the Satimo StarLab system. Results show that the MIMO antenna has a measured dual band of 2.4–2.48 and 5.15–5.8 GHz with the efficiencies of more than 40%, which is higher than any other transparent antennas published in the literature.

**Index Terms**—High efficiency, high gain, multiple-input-multiple-output (MIMO), transparent antenna, wireless local area network (WLAN).

## I. INTRODUCTION

IN THE past two decades, the design of transparent antennas has attracted much attention [1]–[6]. The first transparent microstrip-line-fed patch antenna was reported in NASA's technical memorandum in 1997 [1]. Recently, a dual-band transparent antenna with coplanar-waveguide-feed for active radio frequency identification tags operating at 2.45 and 5.8 GHz has been studied in [2]. Hot soldering could easily damage the transparent-conducting film (TCF) used to fabricate transparent antennas. A novel and a nonthermal soldering method was proposed in [3]. Most transparent antennas studied so far used the transparent conductive silver-coated polyester films (AgHT-8 or AgHT-4) as the conducting materials, which have high sheet resistances of 4–8  $\Omega/\text{sq}$ . The high sheet resistances lead to low radiation efficiencies of the transparent antennas. For example, in [3] and [4], the efficiencies of the transparent antennas achieved were lower than 20%, making the antennas not quite practical to use.

Manuscript received June 23, 2016; revised September 1, 2016; accepted September 23, 2016. Date of publication September 29, 2016; date of current version April 17, 2017.

The authors are with the Department of Electrical and Electronic Engineering, The University of Hong Kong, Hong Kong (e-mail: qlli@eee.hku.hk; swcheung@eee.hku.hk; diwu@eee.hku.hk; tiyuk@eee.hku.hk).

Color versions of one or more of the figures in this letter are available online at <http://ieeexplore.ieee.org>.

Digital Object Identifier 10.1109/LAWP.2016.2614577

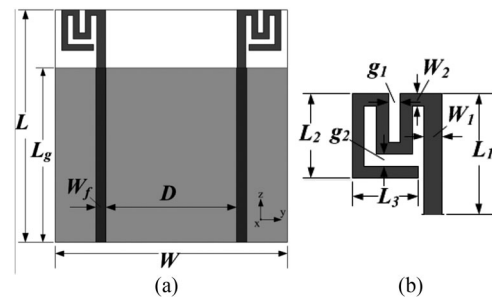


Fig. 1 Geometries of (a) proposed antenna and (b) radiating element (the conductive layer on the top side and the conductive layer on the bottom side).

The IEEE 802.11 standard, which is also known as the wireless local area network (WLAN), has become the most popular network for accessing the internet [7]–[9]. Multiple-input-multiple-output (MIMO) technology, implemented by installing multiple antennas at the transmitter and receiver, can improve the quality and channel capacity of wireless communications systems [10], [11], and so it has been included in the specification of WLAN. MIMO antennas for WLAN systems are mainly designed using copper conductors [7]–[9]. Transparent antennas would have a great future potential if they could be used on a smartphone screen with high efficiency and gain.

In this letter, an optically transparent dual-band MIMO antenna having high efficiency and gain fabricated on a glass substrate for the WLAN system is presented. The TCF used in the design is a micro-metal mesh conductive (MMMC) film constructed by Cima NanoTech using SANTE self-assembling nanoparticle technology [12] and having a sheet resistance of  $0.05 \Omega/\text{sq}$ , much lower than 8 and 4  $\Omega/\text{sq}$  offered by AgHT-8 and AgHT-4, respectively. The MMMC film has a high transmittance of more than 75%, making it suitable to be integrated on a smartphone screen, in building windows, car windows, and solar photovoltaic panels. This type of TCF has never been used to design antennas before. It was once used to design a transparent 3-dB branch-line coupler in [13]. Results show that the proposed antenna can achieve efficiency of more than 40%, much higher than 20% in the previous transparent antennas using AgHT-8 and AgHT-4 [3], [4].

## II. ANTENNA DESIGN

The geometry of the proposed transparent dual-band MIMO antenna is shown in Fig. 1. It consists of two meandered monopoles on one side of the substrate and a ground plane

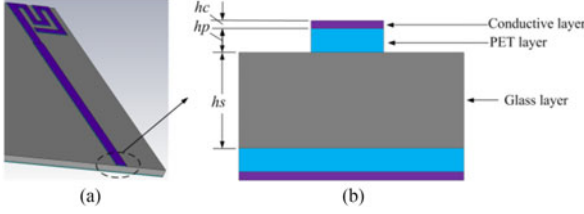


Fig. 2 CST simulation model. (a) Transparent antenna. (b) Cross section of the feedline.

TABLE I  
DIMENSIONS OF PROPOSED ANTENNA (UNIT: mm)

$W$	$W_f$	$W_1$	$W_2$	$L$	$L_g$	$L_1$	$L_2$
40	1.8	1.5	1	40	30	10	7
$L_3$	$D$	$g_1$	$g_2$	$hc$	$hp$	$hs$	—
5.5	22.4	1	1	0.005	0.012	1.09	—

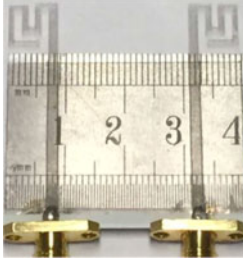


Fig. 3 Prototyped transparent MIMO antenna.

with an area of  $40 \times 30 \text{ mm}^2$  on the other side. Each meandered monopole, as shown in Fig. 1(b), has a length of 31 mm, about  $\lambda_g/4$  at 2.5 GHz and  $3\lambda_g/4$  at 5.6 GHz, where  $\lambda_g$  is the guide wavelength, to generate lower and higher frequency bands for the WLAN system. The two monopoles are separated with a distance of 22.4 mm to reduce mutual coupling and are fed using a 50- $\Omega$  microstrip line with width  $W_f$ . The radiators, feedlines, and ground plane of the antenna are all made of MMMC films. For illustration purpose, the substrate used is a smartphone screen glass with a thickness of 1.09 mm and a relative permittivity of 5.5. The total size of the proposed antenna is  $40 \times 40 \text{ mm}^2$ .

The MMMC film is composed of two layers, a conductive layer made of silver and a polyethylene-terephthalate layer. The dual-band MIMO antenna has been studied and designed using simulation. Fig. 2 shows the simulation model of the antenna and cross section of the feedline using the electromagnetic simulation tool CST. The final parameters of the antenna are listed in Table I, which is used to cut the antenna pattern from an MMMC film. The MMMC antenna pattern is glued on a smartphone glass using a simple nonconductive glue. A conductive glue with a sheet resistance of less than 0.02  $\Omega/\text{sq}$  is used to glue the SMA connectors to the antenna feedlines for measurement. Due to the low sheet resistance, the conductive glue has little effects on the antenna performance. The final prototype is shown in Fig. 3 and used for measurement.

### III. STUDY OF MMMC FILM

The TCF used for the design of the dual-band MIMO antenna is an MMMC film obtained from CIMA [12]. The sheet

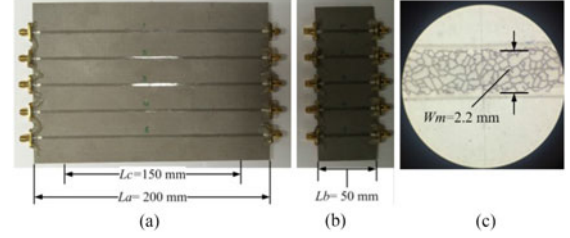


Fig. 4 Prototyped microstrip lines using an MMMC film with (a) length of 200 mm, (b) length of 50 mm, and (c) view through microscope.

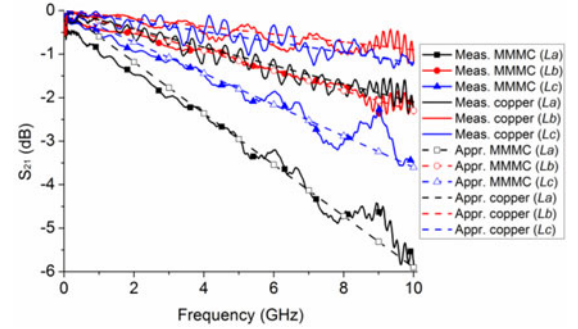


Fig. 5 Measured  $S_{21}$  of microstrip lines with different lengths.

resistance of the film quoted by CIMA is 0.05  $\Omega/\text{sq}$ . In our design, microstrip lines are used to feed the monopoles, as shown in Fig. 1, so it is essential to study the insertion loss of the microstrip feedlines implemented using the MMMC film. To carry out such a study, a Rogers substrate with a thickness of 0.8 mm, a relative permittivity of 2.62, a loss tangent of 0.03, and the copper sheet on one side peeled off, as shown in Fig. 4, is used. The Rogers substrate is cut into two portions, with the areas of  $200 \times 140$  and  $50 \times 140 \text{ mm}^2$ , as shown in Fig. 4(a) and (b), respectively. Five microstrip lines, with a length of  $L_a = 200 \text{ mm}$  and a width of  $W_m = 2.2 \text{ mm}$ , are cut from an MMMC film and glued on the larger substrate, as shown in Fig. 4(a), with enough spacing between adjacent microstrip lines to avoid severe coupling between them. Another five microstrip lines, with a shorter length of  $L_b = 50 \text{ mm}$  and a width of  $W_m = 2.2 \text{ mm}$ , are cut from an MMMC film and glued on the smaller substrate, as shown in Fig. 4(b). The width of 2.2 mm used in these microstrip lines is to make them have a characteristic impedance of 50  $\Omega$  for matching the 50- $\Omega$  SMA connectors. Fig. 4(c) shows a photograph of the microstrip line through a microscope.

For comparison, two copper microstrip lines, with the lengths of  $L_a = 200 \text{ mm}$  and  $L_b = 50 \text{ mm}$  and a width of 2.2 mm, are also fabricated using a Rogers substrate of the same type. All these microstrip lines are connected to SMA connectors using conducting glue for measurement.

The insertion losses ( $S_{21}$ ) of all these microstrip lines have been measured using the vector network analyzer Rohde & Schwarz ZVA 24 in our laboratory. The averages of the measured insertion loss ( $S_{21}$ ) for the five microstrip lines with length  $L_a = 200 \text{ mm}$  and for the other five with  $L_b = 50 \text{ mm}$  are shown in Fig. 2. The insertion losses of the two copper microstrip lines are also measured and shown in Fig. 2. All these results are approximated using straight lines, as shown in Fig. 5. It can be seen that the insertion losses of all these microstrip lines increase with frequency, as expected. The transpar-

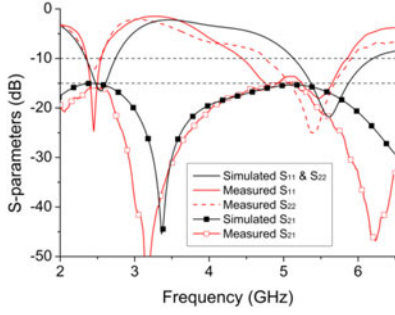


Fig. 6. Simulated and measured  $S$ -parameters.

ent microstrip line with length  $L_a = 200$  mm and  $L_b = 50$  mm have the insertion losses of about 0.58 and 0.23 dB/GHz, respectively, and the copper microstrip lines have the corresponding insertion losses of only about 0.21 and 0.09 dB/GHz.

To reduce the uncertainties caused by the SMA connectors and also the connections using glue between the microstrip lines and the SMA connectors, the insertion loss of only the middle portion, i.e.,  $L_c = 150$  mm in Fig. 2, of the microstrip line is calculated as

$$S_{21}^{Lc} = S_{21}^{La} - S_{21}^{Lb} \quad (1)$$

where  $S_{21}^{La}$  and  $S_{21}^{Lb}$  are the insertion losses (including the SMA connectors and glue connections) for the longer and shorter microstrip lines, respectively. Results are shown in Fig. 5. It can be seen that the transparent microstrip line and the copper microstrip with length  $L_c = 150$  mm have the insertion losses of only 0.35 dB/GHz and 0.12 dB/GHz, respectively. The transparent microstrip lines with  $L_c = 150$  mm has the insertion loss of about 3.5 dB at 10 GHz, and 2 dB at the lower frequencies below 5 GHz. The length of microstrip feedline used in the proposed dual-band MIMO antenna of Fig. 1 is 30 mm, so the insertion loss due to the use of an MMC film is less than 1 dB. The copper microstrip with the same length has the insertion loss of less than 1.2 dB across the tested frequency band from 0 to 10 GHz. Thus, at frequency of less than 5 GHz, the difference in insertion loss between using copper and MMC film to fabricate a microstrip line with a length of 150 mm is less than 1.3 dB.

#### IV. SIMULATION AND MEASUREMENT RESULTS

The simulated and measured  $S$ -parameters of the proposed transparent MIMO antenna are shown in Fig. 6. When one port is being studied, the other port is terminated with a 50- $\Omega$  matching load. Note that since the antenna is symmetrical, the simulated  $S_{11}$  and  $S_{22}$  are identical. The simulated impedance bandwidths for ports 1 and 2, for  $S_{11}$  and  $S_{22} < -10$  dB, for the lower and higher frequency bands are 2.36–2.74 and 5.14–6.18 GHz, respectively. The measured bandwidths for the lower frequency bands are 2.36–2.54 and 2.35–2.53 GHz for ports 1 and 2, respectively, which are slightly narrower than the simulated results. The measured bandwidths for the higher frequency bands are 4.45–5.86 and 4.76–5.9 GHz for ports 1 and 2, respectively, which are slightly wider than the simulated results. The discrepancies between simulation and measurement are mainly due to the fabrication and measurement tolerances. Both the simulated and measured results can cover the required frequency bands of 2.4–2.48 and 5.15–5.8 GHz for the WLAN system. Mutual

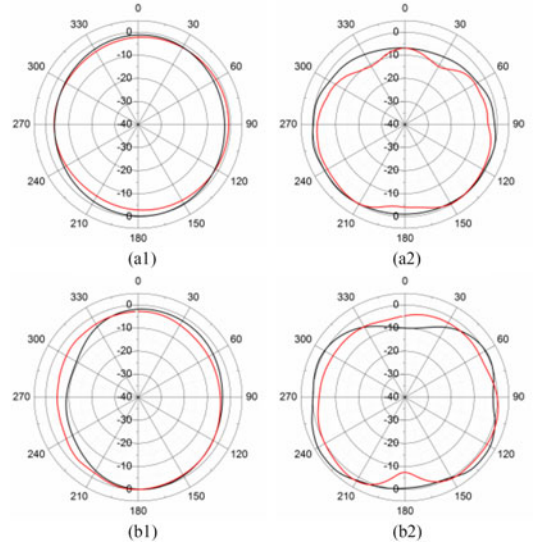


Fig. 7. Simulated and measured radiation patterns with port 1 excited and port 2 terminated with 50- $\Omega$  load: (a1) and (a2) at 2.44 GHz, and (b1) and (b2) at 5.5 GHz. (simulated, measured). (a1)  $xy$ -plane; (a2)  $xz$ -plane; (b1)  $xy$ -plane; (b2)  $xz$ -plane.

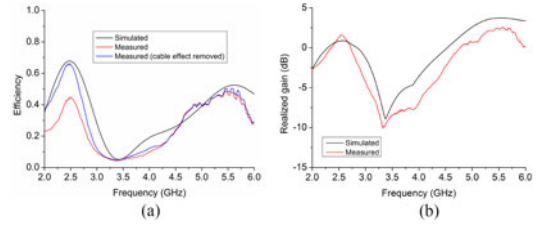


Fig. 8. Simulated and measured (a) efficiencies and (b) realized peak gains.

coupling between the two ports is indicated by  $S_{21}$  in Fig. 5. It can be seen that mutual coupling in both the lower and higher WLAN bands of 2.4–2.48 and 5.15–5.8 GHz, respectively, is lower than  $-15$  dB, enough for good performances in MIMO applications [14].

The radiation patterns of realized gain for the MIMO antenna have been studied using simulation and measurement. Due to the symmetrical structure, the radiation patterns of the antenna with either ports excited are mirror images of each other along the  $xz$ -plane, so only the results with port 1 excited and port 2 terminated with a 50- $\Omega$  matching load are presented here. The simulated and measured radiation patterns of the MIMO antenna at 2.44 and 5.5 GHz (the center frequencies in both bands) are shown in Fig. 7. Good agreements can be observed. At both 2.44 and 5.5 GHz, the antenna has omnidirectional radiation patterns in the  $xy$ - and  $xz$ -planes, as shown in Fig. 7, typical for monopole.

The simulated and measured efficiencies and realized peak gains of the antenna are shown in Fig. 8. The measured efficiency is the average of the measured efficiencies for ports 1 and 2. In Fig. 8(a), it can be seen that the simulated and measured efficiencies agree well in the higher band, with the simulated efficiency slightly higher than the measured result. However, in the lower band, the simulated efficiency is much higher than the measured result. This is mainly due to the feeding cable used in measurement [15], which can be explained as follows. In simulation, a feeding cable is not needed to feed the signal to the antenna. However, in measurement, a coaxial feeding cable



TABLE II  
COMPARISON OF PROPOSED TRANSPARENT ANTENNA WITH OTHER WORKS

Ref.	TCF used	Efficiency	Peak gain (dBi)
[2]	AgHT-8 (8 $\Omega$ /sq)	Not mention	−3.25 (2.45 GHz) −4.53 (5.8 GHz)
[3]	AgHT-8 (8 $\Omega$ /sq)	18% (4 GHz) 17% (8 GHz)	−4 (4 GHz) −2.5 (8 GHz)
[4]	AgHT-8 (8 $\Omega$ /sq)	15% (4 GHz) 18% (8 GHz)	−5.5 (4 GHz) −6 (8 GHz)
[5]	AgHT-4 (4 $\Omega$ /sq)	Not mention	−5 (2 GHz) −20 (4 GHz) −5 (6 GHz)
[6]	AgHT-8 (8 $\Omega$ /sq)	Not mention	−3.5 (5 GHz) −4.7 (15 GHz) −4.8 (25 GHz)
Proposed	MMMC (0.05 $\Omega$ /sq)	43% (2.44 GHz) 46% (5.5 GHz)	0.74 (2.44 GHz) 2.30 (5.5 GHz)

is used to connect the antenna to the measurement system. At low frequencies when the ground plane of the MIMO antenna becomes electrically small compared to the wavelength, current will flow back from the antenna to the surface of the feeding cable, leading to radiation [16] that affects the measured radiation pattern. To reduce the effects, the feeding cable provided by Satimo for use in the StarLab system is covered with electromagnetic suppressant tubing to absorb radiation. As a result, the measured efficiency will be lower than the actual value. To study this cable effect, the simulation model of the feeding cable developed in [14] has been included in simulation. The difference between the simulated efficiencies with and without using the cable model is the effect caused by the cable and is used to remove the cable effect in the measured efficiency. The final results are shown in Fig. 8(a) for comparison. It can be seen that the simulated efficiency and the measured efficiency with the simulated cable effect removed agree much better in the lower band. Note that cable effect only exists in measurement. When the antenna is used in practice, no feeding cable is needed, and hence there is no cable effect. The simulated realized peak gain and measured realized peak gain are shown in Fig. 8(b). The cable effects in the realized peak gain cannot be removed as in the efficiency as explained in [15], and thus is not shown. It can be seen that the measured realized gain and the simulated realized gain agree very well. The measured realized gain ranges from 0.35 to 1.15 dBi in the lower frequency band of 2.4–2.48 GHz and 1.19–2.57 dBi in the higher frequency band of 5.15–5.8 GHz.

We compare the efficiency and realized peak gain of our proposed antenna to those of other transparent antennas in [2]–[6] using other TCF, and results are listed in Table II.

It can be seen that the low efficiencies and realized peak gains of other transparent antennas, due to the use of TCF with high sheet resistances, are too small for practical uses. The proposed transparent antenna, using the MMMC film with a sheet resistance of 0.05  $\Omega$ /sq, can achieve the efficiencies of 43% and 46% and the realized peak gains of 0.74 and 2.30 dBi, at 2.44 and 5.5 GHz, respectively. These values are much higher than those achieved using other TCFs.

## V. CONCLUSION

A transparent dual-band MIMO antenna designed using the MMMC film for the WLAN system has been presented. The antenna consists of two symmetric meandered monopoles on a transparent glass with the bottom side covered by a layer of the MMMC film serving as ground. The MIMO antenna has been studied using simulation and measurement. Results have showed that the MIMO antenna has the bandwidths enough to cover the required operating frequency bands of 2.4–2.48 and 5.15–5.8 GHz, with the efficiencies and realized peak gains much higher than those obtained in previous works.

## REFERENCES

- [1] R. N. Simons and R. Q. Lee, "Feasibility study of optically transparent microstrip patch antenna," in *Proc. Int. Symp. Radio Sci. Meeting*, Montreal, QC, Canada, Jul. 1997.
- [2] M. A. Malek, S. Hakimi, S. K. A. Rahim, and A. K. Evizal, "Dual-band CPW-fed transparent antenna for active RFID tags," *IEEE Antennas Wireless Propag. Lett.*, vol. 14, pp. 919–922, 2015.
- [3] T. Peter, R. Nilavalan, H. F. A. Tarboush, and S. W. Cheung, "A novel technique and soldering method to improve performance of transparent polymer antennas," *IEEE Antennas Wireless Propag. Lett.*, vol. 9, pp. 918–921, 2010.
- [4] T. Peter, Y. Y. Sun, T. I. Yuk, H. F. A. Tarboush, R. Nilavalan, and S. W. Cheung, "Miniature transparent UWB antenna with tunable notch for green wireless applications," in *Proc. Int. Workshop Antenna Technol.*, 2011, pp. 259–262.
- [5] A. Katsounaros, Y. Hao, N. Collings, and W. A. Crossland, "Optically transparent ultra-wideband antenna," *Electron. Lett.*, vol. 45, pp. 722–723, 2009.
- [6] S. Hakimi, S. K. A. Rahim, M. Abedian, S. M. Noghabaei, and M. Khalily, "CPW-fed transparent antenna for extended ultrawideband applications," *IEEE Antennas Wireless Propag. Lett.*, vol. 13, pp. 1251–1254, 2014.
- [7] W. J. Liao, S. H. Chang, J. T. Yeh, and B. R. Hsiao, "Compact dual-band WLAN diversity antennas on USB dongle platform," *IEEE Trans. Antennas Propag.*, vol. 62, no. 1, pp. 109–118, Jan. 2014.
- [8] M. S. Khan, M. F. Shafique, A. Naqvi, A. D. Capobianco, B. Ijaz, and B. D. Braaten, "A miniaturized dual-band MIMO antenna for WLAN applications," *IEEE Antennas Wireless Propag. Lett.*, vol. 14, pp. 958–961, 2015.
- [9] Z. Wen, L. Liu, S. W. Cheung, and Y. F. Cao, "Dual-band MIMO antenna using double-T structure for WLAN applications," in *Proc. 2014 Int. Workshop Antenna Technol.*, 2014, pp. 232–235.
- [10] L. Zheng and N. C. Tse, "Diversity and multiplexing: A fundamental tradeoff in multiple-antenna channels," *IEEE Trans. Inf. Theory*, vol. 49, no. 5, pp. 1073–1096, May 2003.
- [11] G. J. Foschini and M. J. Gans, "On limits of wireless communication in a fading environment when using multiple antennas," *Wireless Pers. Commun.*, vol. 6, no. 3, pp. 311–335, 1998.
- [12] (2016). [Online]. Available: <http://www.cimananotech.com>
- [13] B. M. Sa'ad *et al.*, "Transparent branch-line coupler using micro-metal mesh conductive film," *IEEE Microw. Wireless Compon. Lett.*, vol. 24, no. 12, pp. 857–859, Dec. 2014.
- [14] L. Liu, S. W. Cheung, and T. I. Yuk, "Compact MIMO antenna for portable devices in UWB applications," *IEEE Trans. Antennas Propag.*, vol. 61, no. 8, pp. 4257–4264, Aug. 2013.
- [15] L. Liu, S. W. Cheung, Y. F. Weng, and T. I. Yuk, "Cable effects on measuring small planar UWB monopole antennas," in *Ultra Wideband—Current Status and Future Trends*, M. A. Matin, Ed. Rijeka, Croatia: InTech, Oct. 2012.
- [16] C. Icheln, "Methods for measuring RF radiation properties of small antennas," Ph.D. dissertation, Dept. Elect. Commun. Eng., Espoo, Finland: Helsinki Univ. Technol., Nov. 2001.